Single-Carrier HARQ Using Joint THP and FDE

Kazuki TAKEDA† Hiromichi TOMEBA† and Fumiyuki ADACHI‡
Dept. of Electrical and Communications Engineering, Graduate School of Engineering, Tohoku University
6-6-05 Aza-Aoba, Aramaki, Aoba-ku, Sendai, 980-8579 Japan
†{kazuki, tomeba}@mobile.ecei.tohoku.ac.jp ‡adachi@ecei.tohoku.ac.jp

***Abstract*—In the next generation mobile communication systems, high-speed and high-quality packet data services are demanded. Hybrid ARQ (HARQ) is known as one of the promising error control techniques for wireless packet transmission. However, in a severe frequency-selective fading channel, the single-carrier (SC) HARQ throughput performance degrades due to inter-symbol interference (ISI). In this paper, we consider joint Tomlinson-Harashima precoding (THP) and frequency-domain equalization (FDE) to obtain the frequency-diversity gain while suppressing the residual ISI after FDE. We evaluate, by computer simulation, the SC HARQ throughput performance using joint THP/FDE in a frequency-selective Rayleigh fading channel.**

Keywords-components; Single-carrier, hybrid ARQ, Tomlinson-Harashima precoding, frequency-domain equalization

I. INTRODUCTION

For the next generation mobile communication systems, high-speed and high-quality packet data services are demanded. Turbo coded hybrid ARQ (HARQ) is known as one of the promising error control techniques to realize the high-speed wireless packet access systems [1]. The use of high level modulation is essential [2]. However, the data transmission using high level modulation is vulnerable to the channel distortion. The distortion is produced by the fact that the channel is composed of many propagation paths having different time delays. The single-carrier (SC) transmission performance significantly degrades due to inter-symbol interference (ISI) [3]. Frequency-domain equalization (FDE) based on the minimum mean square error (MMSE) criterion can significantly improve the bit error rate (BER) performance of SC transmission [4-6]. However, the residual ISI after FDE limits the performance improvement, particularly when higher level modulation (e.g., 16QAM, 64QAM) is used. ISI cancellation techniques have been intensively studied to improve the BER performance of SC transmission using FDE [7, 8]. However, the use of ISI cancellation techniques increases the receiver computational complexity.

Recently, Tomlinson-Harashima precoding (THP) [9, 10] has been attracting much attention as an effective technique to suppress the ISI [11, 12]. Although THP requires the channel state information (CSI), THP can suppress the ISI without increasing the complexity of the receiver. Recently, we proposed a joint use of THP and FDE for SC transmission [13]. In our proposed scheme, THP is used to suppress the residual ISI after FDE. Assuming the perfect knowledge of CSI at both the transmitter and receiver, the residual ISI can be completely removed and the BER performance of SC transmission using high-level modulation can be significantly improved.

In HARQ system, error correction coding is indispensable. However, application of joint THP/FDE to turbo coded SC transmission is not simple. Log likelihood ratio (LLR) associated with each bit is required as the soft decision variable for turbo decoding. In this paper, we present the computation method of LLR for turbo decoding when using THP, and evaluate the throughput performance by computer simulation.

The rest of the paper is organized as follows. Sec. II presents the transmission system model of SC HARQ with joint THP/FDE. In Sec. III, the throughput performance of SC HARQ with joint THP/FDE is evaluated by computer simulation. Sec. IV concludes the paper.

II. HARQ WITH JOINT THP/FDE

In this paper, a symbol-spaced discrete-time representation is used. At first, we will present the transmission system model when using joint THP/FDE in Sec. II A. Next, LLR computation for turbo decoding will be presented in Sec. II B. In Sec. II C, the principle operation of HARQ type II S-P8 will be given.

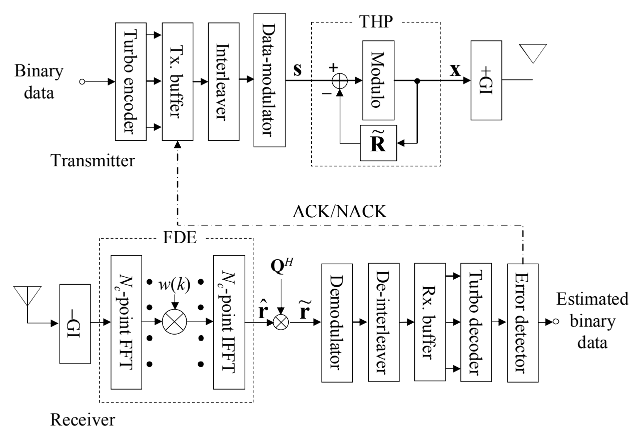

Fig. 1 SC HARQ with joint THP/FDE.

A. *Transmission system model* [13]

Fig. 1 illustrates the SC HARQ transmission system model using joint THP/FDE. The data symbol block to be transmitted can be represented using the vector form as $\mathbf{s}=[s(0), \ldots, s(N_c-1)]^T$, where N_c is the block size of fast Fourier transform (FFT). THP transforms an N_c-symbol vector $\mathbf{s}$ into a signal vector $\mathbf{x}=[x(0), \ldots, x(N_c-1)]^T$. $\mathbf{x}$ can be expressed as

$$\mathbf{x} = \mathbf{s} - \tilde{\mathbf{R}}\mathbf{x} + 2M\mathbf{z}_t \ , \quad (1)$$

where the matrix $\tilde{\mathbf{R}}$ is the feedback coefficient matrix of THP. The (i, j)th component of $\tilde{\mathbf{R}}$ is given by

$$\widetilde{\mathbf{R}}_{i,j}=\begin{cases}\mathbf{R}_{i,j}/\mathbf{R}_{i,i}, & i<j\\ 0, & i\geq j\end{cases}, \tag{2}$$

where $\mathbf{R}$ is an upper triangular matrix (which is given by Eq. (11)). $2M\mathbf{z}_t=[2Mz_t(0), \ldots, 2Mz_t(N_c-1)]^T$ represents the modulo operation [14] at the transmitter. The modulo operator is applied to the real and imaginary parts of the input signal so that they are limited within a range of $[-M, M)$. After the insertion of an N_g-sample guard interval (GI), $\mathbf{x}$ is transmitted.

The transmitted signal vector $\mathbf{x}$ propagates the channel and is received at the receiver. The channel between the transmitter and the receiver is assumed to be an L-path frequency-selective block fading channel. The impulse response of the channel is expressed as

$$h(\tau)=\sum\nolimits_{l=0}^{L-1}h_l(\tau-\tau_l), \tag{3}$$

where h_l and τ_l are respectively the complex-valued path gain with $\sum\nolimits_{l=0}^{L-1}E[|h_l|^2]=1$ and the time delay of the lth path. In this paper, we assume $\tau_l=l$. The received signal block in the time-domain can be represented using the vector form as

$$\mathbf{r}=[r(0), \ \ldots, \ r(N_c-1)]^T=\sqrt{2E_s/T_s}\,\mathbf{h}\mathbf{x}+\mathbf{n}, \tag{4}$$

where E_s and T_s respectively denote the average transmit energy per symbol and the symbol duration, $\mathbf{h}$ is the channel matrix, and $\mathbf{n}=[n(0), \ldots, n(N_c-1)]^T$ is the noise vector. $\mathbf{h}$ is represented as

$$\mathbf{h}=\begin{bmatrix} h_0 & & & \ddots & \vdots \\ \vdots & \ddots & & \mathbf{0} & h_{L-1} \\ h_{L-1} & & h_0 & & \\ & \ddots & \vdots & \ddots & \\ \mathbf{0} & & h_{L-1} & \cdots & h_0 \end{bmatrix}. \tag{5}$$

$n(t)$ is a zero-mean additive white Gaussian noise (AWGN) having the variance $2N_0/T_s$ (N_0 is the one-sided power spectrum density).

The received signal is first transformed into a frequency-domain signal for performing FDE. After FDE, the received signal is transformed back to the time-domain signal. The time-domain received signal vector $\hat{\mathbf{r}}$ after FDE can be expressed as [13]

$$\hat{\mathbf{r}}=[\hat{r}(0), \ \ldots, \ \hat{r}(N_c-1)]^T=\sqrt{2E_s/T_s}\,\hat{\mathbf{h}}\mathbf{x}+\hat{\mathbf{n}}, \tag{6}$$

where $\hat{\mathbf{h}}$ is the equivalent channel matrix and $\hat{\mathbf{n}}=[\hat{n}(0), \ldots, \hat{n}(N_c-1)]^T$ is the noise vector after FDE. $\hat{\mathbf{h}}$ is given as

$$\hat{\mathbf{h}}=\begin{bmatrix} \hat{h}_0 & \hat{h}_1 & \hat{h}_2 & \cdots & \hat{h}_{-1} \\ \hat{h}_{-1} & \hat{h}_0 & \hat{h}_1 & \hat{h}_2 & \\ & \ddots & \ddots & \ddots & \\ \hat{h}_2 & \cdots & \hat{h}_{-1} & \hat{h}_0 & \hat{h}_1 \\ \hat{h}_1 & \hat{h}_2 & \cdots & \hat{h}_{-1} & \hat{h}_0 \end{bmatrix} \tag{7}$$

with

$$\hat{h}_l=\frac{1}{N_c}\sum_{k=0}^{N_c-1}H(k)w(k)\exp\left(-j2\pi k\frac{l}{N_c}\right), \tag{8}$$

where $H(k)$ and $w(k)$ respectively denote the channel gain and FDE weight. $H(k)$ is given by

$$H(k)=\sum_{l=0}^{L-1}h_l\exp\left(-j2\pi k\frac{\tau_l}{N_c}\right). \tag{9}$$

The equivalent channel matrix given by Eq. (7) is not a diagonal matrix and therefore the residual ISI is produced. To suppress the residual ISI after FDE, we use THP at the transmitter. However, since the equivalent channel is a non-causal channel, THP cannot be used directly. To use THP, we apply QR-decomposition [15] to $\hat{\mathbf{h}}$ in order to transform the non-causal equivalent channel into a causal channel. Using a unitary matrix $\mathbf{Q}$ and an upper triangular matrix $\mathbf{R}$, $\hat{\mathbf{h}}$ can be expressed as

$$\hat{\mathbf{h}}=\mathbf{Q}\mathbf{R}. \tag{10}$$

Multiplying the received signal vector $\hat{\mathbf{r}}$ by the Hermetian transposition of the unitary matrix $\mathbf{Q}$ gives

$$\widetilde{\mathbf{r}}=\mathbf{Q}^H\hat{\mathbf{r}}=\sqrt{2E_s/T_s}\,\mathbf{R}\mathbf{x}+\mathbf{Q}^H\hat{\mathbf{n}}. \tag{11}$$

Substituting Eq. (1) into (11), $\widetilde{\mathbf{r}}$ can be rewritten as

$$\widetilde{\mathbf{r}}=\sqrt{\frac{2E_s}{T_s}}\begin{bmatrix} R_{0,0} & & \mathbf{0} \\ & \ddots & \\ \mathbf{0} & & R_{N_c-1,N_c-1} \end{bmatrix}(\mathbf{s}+2M\mathbf{z}_t)+\mathbf{Q}^H\hat{\mathbf{n}}, \tag{12}$$

which is input to the same modulo operator used in the transmitter to obtain the decision variable. The output of the modulo operator can be expressed as

$$\hat{\mathbf{s}}=\mathbf{s}+2M(\mathbf{z}_t+\mathbf{z}_r)+\left(\frac{2E_s}{T_s}\right)^{-\frac{1}{2}}\begin{bmatrix} R_{0,0}^{-1} & & \mathbf{0} \\ & \ddots & \\ \mathbf{0} & & R_{N_c-1,N_c-1}^{-1} \end{bmatrix}\mathbf{Q}^H\hat{\mathbf{n}}, \tag{13}$$

where $2M\mathbf{z}_r=[2Mz_r(0), \ldots, 2Mz_r(N_c-1)]^T$ represents the modulo operation at the receiver and the first, second, and third terms respectively denote the desired signal, modulo operation, and noise. If the noise can be neglected, $2M\mathbf{z}_r\approx-2M\mathbf{z}_t$ and the transmitted data symbol vector $\mathbf{s}$ is recovered without causing distortion at the receiver.

It was shown in [4] that when FDE is used alone, the best BER performance can be achieved by MMSE-FDE. However, for joint use of THP, the use of equal gain combining (EGC)-FDE provides the best BER performance, which is better than that achievable by "MMSE-FDE only" [13]. Below, we discuss why joint THP/EGC-FDE can provide better BER performance than joint THP/MMSE-FDE or maximum ratio combining (MRC)-FDE. If the residual ISI after FDE can be completely removed, MRC-FDE provides the best BER performance. Joint THP/FDE can suppress the residual ISI after FDE completely; however, QR-decomposition is performed on the equivalent channel matrix and the strong correlation between two column vectors of $\hat{\mathbf{h}}$ reduces the squared value of the diagonal components of **R**, which is the signal power. Although MRC-FDE can provide the largest SNR after FDE, the correlation is stronger for MRC than for EGC and MMSE. Therefore, the signal power significantly degrades. Since the equivalent channel matrix of MMSE-FDE is close to the diagonal matrix, the signal power loss due to QR-decomposition is small; however, the SNR after FDE is lower than MRC and EGC. On the other hand, EGC can achieve the SNR close to MRC when using FDE only and furthermore, the power loss due to QR-decomposition is smaller than that of MRC. As a consequence, joint THP/EGC-FDE provides the best BER performance. In this paper, for joint THP/FDE, we use the EGC-FDE weight given as

$$w(k) = H^*(k)/|H(k)|. \tag{14}$$

B. LLR computation for turbo decoding

The log-likelihood ratio (LLR) is computed as the soft decision variable for turbo decoding [16, 17]. From Eq. (13), LLR of the bit b belonging to the tth symbol is given by

$$L_b = \ln \frac{p(\hat{s}(t)|\{\tilde{s}:b=1\})}{p(\hat{s}(t)|\{\tilde{s}:b=0\})}, \tag{15}$$

where $\{\tilde{s}:b=0 \text{ or } 1\}$ is a set of symbols with the bit b of interest being b=0 or 1. We compute the LLR using $\tilde{\mathbf{r}}$. The conditional probability density function $p(\tilde{r}(t)|\{\tilde{s}:b=0 \text{ or } 1\})$ is expressed as

$$p(\tilde{r}(t)|\{\tilde{s}:b=0 \text{ or } 1\}) = \sum_{n=0}^{N/2-1}\sum_{x_n}\sum_{y_n} \frac{1}{\sqrt{2\pi}\sigma(t)}\exp\left(-\frac{\left|\tilde{r}(t)-\sqrt{2E_s/T_s}R_{t,t}(\tilde{s}_n+2M\tilde{z}_{n,x_n,y_n})\right|^2}{2\sigma^2(t)}\right), \tag{16}$$

where N is the number of symbol candidates, $\tilde{s}_n (\in \{\tilde{s}:b=0 \text{ or } 1\}, n=0\sim N/2-1)$ is a candidate symbol with the bit b of interest being b=0 or 1. To remove the distortion introduced by the modulo operation at the transmitter, $\{2M\tilde{z}_{n,x_n,y_n}=2M(x_n+jy_n);\ x_n,\ y_n=0,\pm1,\pm2,\ldots\}$ is introduced. $\sigma^2(t)$ is the noise power given as

$$\sigma^2(t) = \frac{N_0}{T_s}\sum_{k=0}^{N_c-1}|w(k)|^2\left|\sum_{i=0}^{N_c-1}Q_{i,t}\exp\left(-j2\pi k\frac{i}{N_c}\right)\right|^2. \tag{17}$$

Eq. (16) can be approximated as

$$\begin{aligned} p(\tilde{r}(t)|\{\tilde{s}:b=0 \text{ or } 1\}) &\approx \sum_{n=0}^{N/2-1}\frac{1}{\sqrt{2\pi}\sigma(t)}\exp\left(-\frac{\left|\tilde{r}(t)-\sqrt{2E_s/T_s}R_{t,t}(\tilde{s}_n+2M\tilde{z}_{n,\min})\right|^2}{2\sigma^2(t)}\right) \\ &\approx \frac{1}{\sqrt{2\pi}\sigma(t)}\exp\left(-\frac{\left|\tilde{r}(t)-\sqrt{2E_s/T_s}R_{t,t}(\tilde{s}_{\min}+2M\tilde{z}_{\min,\min})\right|^2}{2\sigma^2(t)}\right), \end{aligned} \tag{18}$$

where $2M\tilde{z}_{n,\min}$, $2M\tilde{z}_{\min,\min}$, and $\tilde{s}_{\min}$ are given as

$$\begin{cases} \tilde{z}_{n,\min} = \arg\min\limits_{\tilde{z}_{n,x_n,y_n}}\left\{\left|\tilde{r}(t)-\sqrt{2E_s/T_s}R_{t,t}(\tilde{s}_n+2M\tilde{z}_{n,x_n,y_n})\right|^2\right\} \\ \tilde{z}_{\min,\min} = \arg\min\limits_{\tilde{z}_{n,\min}}\left\{\left|\tilde{r}(t)-\sqrt{2E_s/T_s}R_{t,t}(\tilde{s}_n+2M\tilde{z}_{n,\min})\right|^2\right\} \\ \tilde{s}_{\min} = \arg\min\limits_{\tilde{s}_n}\left\{\left|\tilde{r}(t)-\sqrt{2E_s/T_s}R_{t,t}(\tilde{s}_n+2M\tilde{z}_{n,\min})\right|^2\right\} \end{cases}. \tag{19}$$

Hence, the LLR of the bit b belonging to the tth symbol can be computed from [16]

$$\begin{aligned} L_b &= \ln\frac{p(\tilde{r}(t)|\{\tilde{s}:b=1\})}{p(\tilde{r}(t)|\{\tilde{s}:b=0\})} \\ &\approx \frac{\left|\tilde{r}(t)-\sqrt{2E_s/T_s}R_{t,t}(\tilde{s}_{\min}^{b=0}+2M\tilde{z}_{\min,\min}^{b=0})\right|^2}{2\sigma^2(t)} - \frac{\left|\tilde{r}(t)-\sqrt{2E_s/T_s}R_{t,t}(\tilde{s}_{\min}^{b=1}+2M\tilde{z}_{\min,\min}^{b=1})\right|^2}{2\sigma^2(t)}. \end{aligned} \tag{20}$$

Turbo decoding is carried out using the LLR sequence.

As an example, the Euclidian distance between $\tilde{r}(t)$ and $s(t)+2Mz_t(t)$ for 16QAM (four bits in one symbol) is discussed below. $\tilde{r}(t)$ is represented by "x" and the symbol candidates are represented by "●, ○". Eq. (16) indicates that the Euclidian distance between $\tilde{r}(t)$ and $\{\tilde{s}_n+2M\tilde{z}_{n,x_n,y_n}\}$ is needed for all n. The candidate symbols are distributed over the entire area due to the modulo operation at the transmitter. However, the true candidate symbols indicated by "●" are present only in the square area whose center is indicated by "x" and the other symbols indicated by "○" are images of true ones. The LLRs for four bits in the 16QAM symbol can be calculated using Eq. (20) by using 16 candidates indicated by "●".

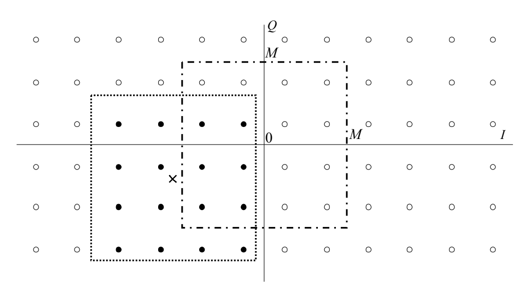

Fig. 2 Received signal constellation for 16QAM.

C. *HARQ Type II S-P8* [18]

In this paper, HARQ type II S-P8 [18] shown in Fig. 3 is considered. Turbo coding with rate R=1/3 is considered. The turbo encoder outputs the systematic bit sequence and two parity bit sequences. These sequences are punctured into nine sequences (including systematic bit sequence) by the puncturing matrices indicated by octal notation as shown in Fig. 3.

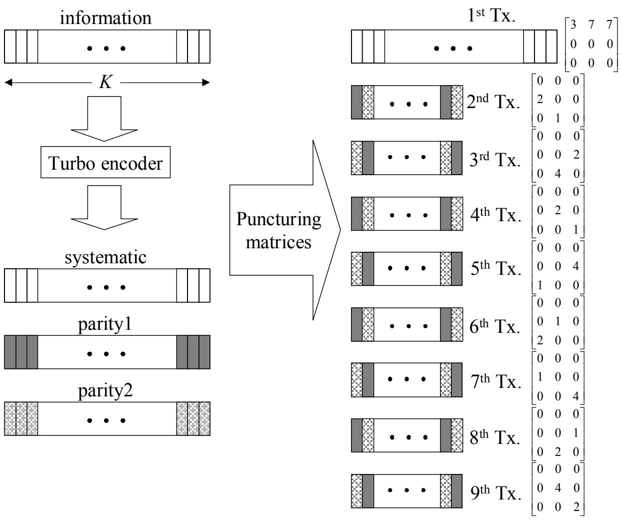

Fig. 3 HARQ type II S-P8.

For the first transmission, only the systematic bit sequence is transmitted. At the receiver, data decision and error detection are performed. If any error is detected in the received packet, second transmission is requested from the receiver by sending an NACK signal. When the NACK signal is received at the transmitter, the second packet (consisting of the punctured parity bit sequence) is transmitted. At the receiver, turbo decoding is carried out by using the first and second received packets. If any error is detected after turbo decoding, the NACK signal is transmitted again. One of the punctured parity bit sequences is transmitted each time the NACK signal is received at the transmitter until the 9th packet transmission. After the 9th packet transmission, the same packet is retransmitted.

With "MMSE-FDE only", when the same packet is retransmitted, the LLR sequence is computed after joint MMSE-FDE and packet combining [16]. However, with joint THP/FDE, since the non-linear modulo operation is performed at the transmitter, packet combining is not easy. In this paper, we apply packet combining based on LLR. When the whole coded sequence has been retransmitted Q times, the LLR of bit b belonging to the tth symbol is computed using

$$L_b = \ln\frac{p(\tilde{r}^0(t),\cdots,\tilde{r}^{Q-1}(t)\,|\{\tilde{s}:b=1\})}{p(\tilde{r}^0(t),\cdots,\tilde{r}^{Q-1}(t)\,|\{\tilde{s}:b=0\})} = \ln\frac{\prod_{q=0}^{Q-1} p(r^q(t)\,|\{\tilde{s}:b=1\})}{\prod_{q=0}^{Q-1} p(r^q(t)\,|\{\tilde{s}:b=1\})} = \sum_{q=0}^{Q-1} L_b^q, \qquad (21)$$

where $\tilde{r}^q(t)$ is the received signal in the qth received packet given by Eq. (12) and L_b^q is given by Eq. (20).

III. Computer Simulation

The simulation condition is summarized in table 1. The information bit length is K=4096. Turbo encoder with coding rate R=1/3 consists of two (13, 15) recursive systematic convolutional (RSC) encoders is used. For turbo decoding, Log-MAP decoding with 8 iterations is used. Ideal channel estimation is assumed. The channel is assumed to be an L=16-path frequency-selective block Rayleigh fading channel with uniform power delay profile ($E[|h_l|^2]$=1/L) [5]. An infinite number of retransmissions is assumed in the simulation.

Table 1 Simulation conditions

Turbo coding	R=1/3 (13, 15)RSC encoder Log-MAP decoding with 8 iterations	
Channel interleaver	Block interleaver	
Data modulation	QPSK, 16QAM, 64QAM, 256QAM	
No. of FFT points	N_c=128	
No. of GI length	N_g=16	
Channel	Frequency-selective block Rayleigh fading	
	No. of paths	L=16
	Power delay profile	Uniform
	Time delay	τ_l=l (l=0~L−1)
ARQ	HARQ type II S-P8	
FDE	EGC	
Channel estimation	Ideal	

The throughput performance with joint THP/FDE is plotted in Fig. 4 as a function of average transmit symbol energy-to-noise power spectrum density ratio E_s/N_0. The throughput performance with "MMSE-FDE only" is also shown. With higher data modulation scheme, the Euclidian distance between the symbol candidates becomes smaller. Therefore, the throughput performance using "MMSE-FDE only" degrades due to the residual ISI after FDE and the noise. On the other hand, joint THP/FDE can perfectly remove the residual ISI after FDE (we are assuming the perfect knowledge of CSI) and can significantly improve the throughput performance in a higher E_s/N_0 region. However, joint THP/FDE uses the modulo operation at the transmitter and therefore data decision is more vulnerable to the noise compared to the conventional MMSE-FDE. This causes the throughput degradation in a lower E_s/N_0 region as seen in Figs. 4 (a) and (b).

Fig. 4 (c) shows the throughput performance with the adaptive modulation scheme. In Fig. 4 (c), the modulation level which gives the best throughput is selected for each E_s/N_0. From this figure, it can be said that the throughput performance is significantly improved in a high E_s/N_0 region by using joint THP/FDE.

IV. Conclusion

To realize the high-speed packet access, the use of higher level modulation is essential. However, with "MMSE-FDE only", the throughput performance degrades due to the residual ISI after FDE. Assuming the perfect knowledge of CSI at both transmitter and receiver, the residual ISI after FDE can be completely removed by using joint THP/FDE. Hence, the joint use of THP and FDE is promising for high-speed packet access. In this paper, we presented a joint use of THP/FDE for turbo coded HARQ transmission. We evaluated the throughput performance of HARQ using joint THP/FDE and have shown that joint THP/FDE significantly improve the throughput performance compared to MMSE-FDE when high level modulation is used. In this paper, we assumed the ideal channel estimation. However, in a real system, the channel estimation error is present and degrades the HARQ throughput performance. The impact of channel estimation error is left as an important future study.

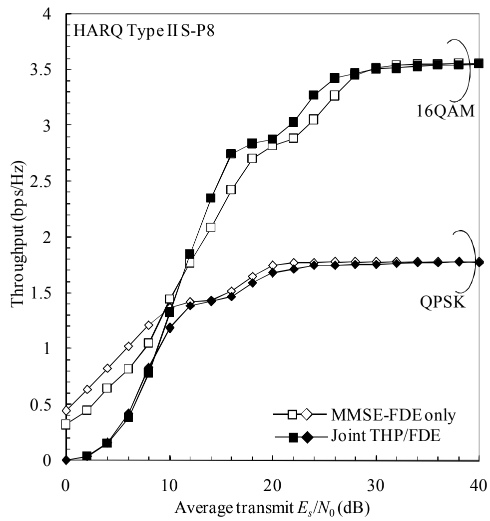

(a) QPSK, 16QAM.

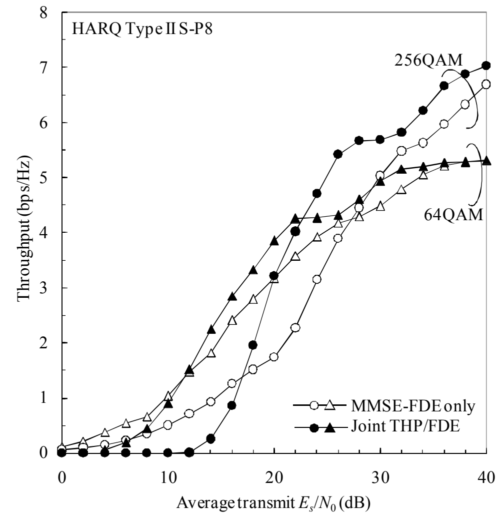

(b) 64QAM, 256QAM.

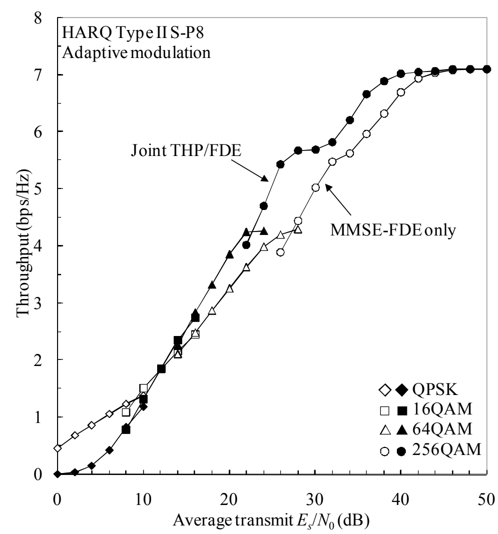

(c) Adaptive modulation.

Fig. 4 Throughput performance of SC HARQ with joint THP/FDE.

REFERENCES

[1] D. N. Rowitch and L. B. Milstein, "Rate compatible punctured turbo (RCPT) codes in hybrid FDE/HARQ system," Proc. Comm. Theory Mini-conference of GLOVECOM'97, pp. 55-59, Nov. 1997.

[2] 3GPP TR25.858, "High speed downlink packet access: physical layer aspects," version 5.0.0.

[3] J. G. Proakis, *Digital communications*, 2nd ed., McGraw-Hill, 1995.

[4] D. Falconer, S. L. Ariyavisitakul, A. Benyamin-Seeyar, and B. Edison, "Frequency-domain equalization for single-carrier broadband wireless systems," IEEE Commun., Mag., Vol. 40, pp. 58-66, Apr. 2002.

[5] Fumiyuki Adachi, Deepshikha Garg, Shinsuke Takaoka, and Kazuaki Takeda, "Broadband CDMA techniques," Special Issue on Modulation, Coding and Signal Processing, IEEE Wireless Commun., Mag., Vol. 12, No. 2, pp. 8-18, Apr. 2005.

[6] Kazuaki Takeda and Fumiyuki Adachi, "Bit error rate analysis of DS-CDMA with joint frequency-domain equalization and antenna diversity reception," IEICE Trans. Commun., Vol. E87-B, No. 10, pp. 2991-3002, Oct. 2004.

[7] S. Tomasin and N. Benvenuto, "A reduced complexity block iterative DFE for dispersive wireless applications," IEEE 60th Vehicular Technology Conference (VTC2004-Fall), Los Angeles, U. S. A, Sept. 2004.

[8] Y. Zhu and K. B. Ketaief, "Single-carrier frequency-domain equalization with decision-feedback processing for time-reversal space-time block coded systems," IEEE Trans. Commun., Vol. 53, No. 7, pp. 1127-1131, Jul. 2005.

[9] M. Tomlinson, "New automatic equalizer employing modulo arithmetic," Electronics Letters, Vol. 7, No. 5/6, pp. 138-139, Mar. 1971.

[10] H. Harashima and H. Miyakawa, "Matched-transmission technique for channels with intersymbol interference," IEEE Trans. Commun., Vol. 20, Nol. 4, pp. 774-780, Aug. 1972.

[11] R. H. Fischer, C. Windpassinger, A. Lampe, and J. Huber, "Space-time transmission using Tomlinson-Harashima precoding," Proc. 4th Itern, ITG conference on source and channel coding, pp. 139-147, Berlin, Jan. 2002.

[12] I. Cosovic, S. Sand, and R. Raulefs, "A non-liner precoding technique for downlink MC-CDMA," IEEE 61st VTC2005-Spring, Stockholm, Sweden, May 30-Jun. 2005.

[13] Kazuki Takeda, Hiromichi Tomeba, and Fumiyuki Adachi, "Single-carrier transmission with joint Tomlinson-Harashima precoding and frequency-domain equalization," The 3rd IEEE VTS Asia Pacific Wireless Communications Symposium, pp. 262-266. Daejoen, Korea, Aug. 2006.

[14] R. Fisher, "The modulo-lattice channel: the key feature in precoding schemes," International Journal of Electronics and Communications, pp. 244-253, Jul. 2005.

[15] Gene. H. Golub, and Charles F. Van Loan, *Matrix computations*, 2nd ed., The Johns Hopkins University Press, 1989.

[16] D. Garg and F. Adachi, "Packet access using DS-CDMA with frequency-domain equalization," IEEE Journal of Select. Areas in Commun., Vol. 24, No. 1, pp. 161-170, Jan. 2006.

[17] A. Stefanov and T. Duman, "Turbo coded modulation for wireless communications with antenna diversity," IEEE 49th VTC99-Fall, pp. 1565-1569, Netherland, Sept. 1999.

[18] J. Hagenauer, "Rate-compatible punctured convolutional codes (RCPT codes) and their application," IEEE Trans. Commun., Vol. 36, No. 4, pp. 389-400, Apr. 1988.